A facile route to improve compatibilization of Low Density PolyEthylene/Poly (ε-caprolactone) blends

Hana Boughrara [a,b], Souad Djelalli [b,c], Nacerddine Haddaoui [b], Jean-Noël Staelens [a], Philippe Supiot [a], and Ulrich Maschke* [a]

[a] Unité Matériaux et Transformations – UMET, UMR 8207, Univ. Lille, CNRS, INRAE, Centrale Lille, F-59000 Lille, France

[b] Laboratoire de Physico-chimie des Hauts Polymères, Département de Génie des Procédés Faculté de Technologie, Université Ferhat Abbas, 19000 Sétif, Algeria

[c] Department of Chemistry, Faculty of Sciences, Université Ferhat Abbas, 19000 Sétif, Algeria

Corresponding author: e-mail: ulrich.maschke@univ-lille.fr

Declarations of interest: none

Abstract

Low density Polyethylene (designated hereafter as "PE") is known for its inactivity, durability and resistance to degradation. For this reason adding pro-oxidants as additives in PE matrix could be efficient to elaborate a material designated as Ox-PE, exhibiting chemical reactivity. This modification could lead to an enhancement of compatibility between Ox-PE and other functionalized polymers. This approach has been exploited in this report to elaborate blends of Ox-PE with poly (ε-caprolactone) (PCL), a biodegradable polymer. Fourier Transform InfraRed spectroscopy (FTIR), Scanning Electron Microscopy (SEM) and thermal characterization by DSC, TGA were applied to investigate structural and thermal properties of PE/PCL (75/25 wt%/wt%) blends, compatibilized with 1 Phr and 5 Phr of Ethylene-co-Glycidyl MethAcrylate (EGMA) copolymer or with a Ox-PE/PCL mixture.

Structural observations of the PE75/PCL25 blend by SEM revealed a phase separated morphology indicating incompatibility between PE and PCL. This was also confirmed by FTIR spectroscopy where no changes were noticed concerning the characteristic bands of either PE or PCL. Incorporating EGMA in the PE75/PCL25 blend resulted in reduced particle sizes of the dispersed PCL phase in the PE matrix confirming the reaction of epoxy groups of EGMA with hydroxyl end-groups of PCL at the interface. Regarding the thermal behavior, all PE/PCL blends exhibited an intermediate response between that of PE and PCL homopolymers. Interestingly, a high degree of compatibility was achieved for the Ox-PE75/PCL25 blend, together with a lower thermal stability compared to PE75/PCL25.

Keywords: Polyethylene (PE); poly (ε-caprolactone) (PCL); Ox-biodegradable Polymer; thermo-oxidation; pro-oxidants additives; compatibilizer.

1. Introduction

Despite the strong development of green polymers in recent years, the use of synthetic polymers has doubled due to their successful application in various domains: packaging, automotive components, transportation, medical equipment, electric, electronic and aerospace parts, among others [1,2]. These materials present good physico-chemical properties such as resistance to corrosion and microbiological attack, insolubility, impermeability towards aqueous media, ensuring their service in different fields [3].

Among the family of polyolefins, low density polyethylene (designated hereafter as "PE") occupies a significant position because of its large tonnage, and its mechanical, thermal and chemical performances, which have enlarged use of PE in a wide range of industrial applications, especially in packaging and agricultural films. However, after this rush of consumption, end-of-life PE accumulates in nature as waste [4].

Consequently, waste accumulation of PE has become a real risk to biodiversity and a source of environmental pollution [5]. The resistance of PE to degradation and biological attacks is attributed mainly to its high molecular weight, hydrophobicity and lack of functional groups on its main chain [6,7]. Indeed, the chemical structure of PE is responsible for its incompatibility with other materials and makes thus the attack by microorganisms difficult, which has a substantial impact on the degradation process [8]. As a result, many research groups proposed different approaches to reduce the accumulation of considerable quantities of non-biodegradable PE waste in the environment [9]. One possible approach consists to blend PE with biodegradable polymers, which could be a notable alternative since each component can contribute by its favorable properties to make the resultant material more interesting [10,11]. In this context, several studies have focused on PE/aliphatic polyester blends such as poly(lactide) (PLA) and poly(hydroxybutyrate-co-valerate) PHBV [12–20]. Nevertheless, only few studies are dealing with the PE/Poly-(caprolactone) (PCL) system despite the

excellent properties that make PCL an outstanding candidate to be blended with polyolefins to achieve specific mechanical and degradation properties [11,21]. PCL is a prominent aliphatic polyester due to its numerous advantages including extraordinary mechanical properties, biocompatibility, hydrophobicity, solubility in several solvents, non-toxicity, and biodegradability [22,23]. Nonetheless, when developing polymer blends, the risk of incompatibility between multiphase components represents a critical factor to be considered. In this context, the most common method for overcoming such a problem is to add compatibilizing agents, such as copolymers containing fragments that are compatible with at least one of the components. Furthermore, interaction between the components at the interface has a significant impact on the morphology of the resulting material, which is a criterion that will determine its final properties [24].

Another interesting way to modify PE structure was recently adopted, based on the incorporation of pro-oxidants or pro-degradants. These additives are usually transition metal-ion complexes in the form of stearates, which may initiate the oxidation of long PE chains in the presence of UV light (photo-oxidation) or heat (thermo-oxidation) [7,25–28]. Cobalt stearate (Co^{2+}), Manganese stearate (Mn^{2+}) and Iron stearate (Fe^{3+}) represent the commonly used pro-oxidant additives with polyolefins [29–34].

Incorporating these compounds facilitates the long PE chain scission leading to the formation of hydrophilic groups, together with a decrease of the molecular weight. The formed fragments, with lower molecular weight and higher hydrophilicity, are more susceptible to be attacked by microorganisms, either in abiotic or biotic environment [35,36].

In this report, the aforementioned approaches were combined to create a blend that poses little environmental risk when discarded after use. Two types of blends have been prepared: (i) blends based on PE/PCL with and without (Ethylene-co-Glycidyl MethAcrylate) (EGMA) as copolymer, and (ii) blends containing Ox-PE (PE with pro-oxidant) and PCL at a fixed

blending ratio of Ox-PE75/PCL25 (wt%/wt%). The physicochemical properties of these blends were assessed using analytical techniques such as Fourier Transform InfraRed spectroscopy (FTIR), Scanning Electron Microscopy (SEM), Differential Scanning Calorimetry (DSC), and Thermo Gravimetric Analysis (TGA).

2. Experimental

2.1. Materials

The low density PE (LDPE 1003/FE/23) was supplied by Total Petrochemicals (Belgium) with a volumetric density of 0.92g/cm^3, a molecular weight (M_w) of 450,000 g/mol, and a melting point of 111°C. Poly(ε-caprolactone) (PCL) (CAPA 6500) was obtained from Perstorp group (Sweden), possessing a M_w~50,000 g/mol and a melting point about 58-60°C. The (ethylene glycidyl methacrylate) (EGMA) copolymer (Lotader) was produced by Arkema group (France). The pro-oxidants used in this study, cobalt stearate, manganese stearate, and iron stearate, were synthesized in our Algerian laboratory according to protocols described in [29] and [31].

2.2. Sample Preparation

2.2.1. PE-PCL-compatibilizer blends

The homopolymers LDPE, PCL were dried at 40°C for 24h. The PE/PCL blends were prepared with different ratios of PCL ranging from 0 to 100 weight% (wt%). The compatibilizer EGMA was added to the PE75/PCL25 blend at two concentrations 1 and 5 Phr. The melt blending for all formulations was carried out at 130°C and 40 rpm for 20 min in a Brabender plasticorder® equipment (Duisburg, Germany).

For simplicity reasons, the designation 75/25 PE/PCL will be used instead of writing 75wt%/25wt% PE/PCL. The PE75/PCL25 blend was selected for two reasons, firstly PE

should present the major part of the mixture to investigate its degradation, and secondly, observations of sample morphology by SEM of this blend showed a continuous PE phase including dispersed PCL spheres as minority phase. EGMA was chosen as compatibilizer following promising results obtained for a PE/polyester system [20]. Applying the PE75/PCL25 blend, low concentrations of EGMA are likely to reduce the size of dispersed nodules and promote compatibility at the interface. The EGMA concentrations applied (1 Phr, 5 Phr) were chosen similar to work on polyolefin/polyester blends [37].

Table 1 describes designation and composition of samples used in this study.

2.2.2. PE/pro-oxidant mixtures

PE was blended with 0.9 Phr of the synthesized pro-oxidants containing 0.3% cobalt stearate, 0.3% of manganese stearate and 0.3% of iron stearate. The melt blending of ingredients was performed in the Brabender plastograph at 140°C and 40 rpm for 10 min. The use of a masterbatch [34], containing the pro-oxidants, presents the advantage to obtain high efficiency compared to the employment of individual pro-oxidants which risk to yield an antagonism effect. The choice of the masterbatch concentration (0.9 Phr) was based on a study of the evolution of the carbonyl level [30], followed by FTIR during 10 days of thermo-oxidation, to detect oxidation products generated by the degradation of PE.

The extrudate of PE/pro-oxidants (Ox-PE) was placed in an air-circulating oven at 70°C for a period of 10 days in order to catalyze the pro-oxidant and accelerate the thermo-oxidation reaction, which is composed of three stages, initiation, propagation and termination [38]. In the first stage, the pro-oxidants undergo thermal decomposition, forming unstable free radicals which subsequently react with hydrogens from PE chains. At the propagation stage, alkyl radicals formed during the previous stage react with atmospheric oxygen to create peroxide radicals, which combine with hydrogens from PE chains leading to the formation of

hydroperoxides and macroradicals. These hydroperoxides decompose thermally, which leads to the formation of new radicals which make it possible to create other oxidation products (alcohols, ketones, carboxylic acids, etc.). The propagation reactions stop when the generated radicals react with each other to give stable species, insensitive to oxidation.

2.2.3. Ox-PE/PCL blends

Blends containing 75wt% of Ox-PE and 25wt% of PCL (Ox-PE75/PCL25) were prepared in the Brabender plastograph at 130°C and 40rpm for 10 min. Thick films (1mm) were prepared from the different formulations using a hydraulic press at a temperature of 160°C.

Table 1

Composition and designation of the prepared samples

Composition and designation	PE (wt %)	PCL (wt %)	EGMA (Phr)	Pro-oxidant (Phr)
PE	100	0	/	/
PE75/PCL25	75	25	/	/
PE50/PCL50	50	50	/	/
PE25/PCL75	25	75	/	/
PCL	0	100	/	/
PE75/PCL25EG1	75	25	1	/
PE75/PCL25EG5	75	25	5	/
Ox-PE75/PCL25	75	25	/	0.9

2.3. Characterization

2.3.1. Fourier Transform Infrared Spectroscopy

FTIR spectra of polymer films were obtained in Attenuated Total Reflection-mode at room temperature in the interval of 500-4000 cm^{-1} using a Perkin Elmer Frontier model with a spectral resolution of 4 cm^{-1} applying 32 scans.

2.3.2. Scanning Electron Microscopy

Fractured surface morphologies of polymer films were observed with a FEI Tecnai 200 kV SEM applying an accelerating voltage of 15 kV and using energy dispersion X-ray analysis. The sample surfaces were coated with a carbon layer to avoid electrostatic charging during analysis.

2.3.3. Differential Scanning Calorimetry

DSC measurements of PE, PCL and the elaborated blends were carried out on a DSC 8000 instrument (Perkin Elmer). The samples were prepared by introducing 8 to 10 mg of the polymers into aluminum pans. Three successive heating and cooling cycles were conducted under nitrogen flow, applying a ramp rate of 10°C/min in the range of temperatures from -70°C to 160°C. Only thermograms of the second heating cycles were taken into account for data analysis. The crystallinity degree (Xc) of samples was calculated using the following equation (1):

$$X_C\ (\%) = (\Delta H_m / W \times \Delta H_{0m})*100 \quad (1)$$

where ΔH_m represents the measured fusion enthalpy, ΔH_{0m} is the fusion enthalpy of 100% crystalline polymers in the blends (PE: 293.1 J/g [39] and PCL : 139.5 J/g [40]), and W stands for the weight fraction of PE and PCL.

2.3.4. Thermogravimetric analysis

TGA and Differential Thermal Analysis (DTA) were performed on a Pyris 1 TGA device (Perkin Elmer) with a resolution of 1µg. Heating of the sample was carried out from 25°C to 700°C with a rate of 10°C/min under nitrogen atmosphere, and a flow rate of 20 mL/min.

4. Results and Discussion

4.1. Structural analysis

Figure 1a represents FTIR spectra of homopolymers PE, PCL and their blends. The spectrum of PE reveals doublets at 2919–2851 cm^{-1} and 1473-1463 cm^{-1}, associated to symmetric and asymmetric (CH_2) stretching and bending deformations of CH_2, respectively. A low absorption band at 1376 cm^{-1} can be attributed to symmetric deformation of methyl groups. A band appearing at 730-719 cm^{-1} corresponds to rocking deformation of methylene groups (CH_2) [41].

In neat PCL, CH_2 groups manifest themselves in several positions: a doublet at 2944-2865 cm^{-1} corresponding to symmetric and asymmetric (CH_2) stretching, and the band at 726 cm^{-1} can be attributed to CH_2 vibration. The intense peak at 1723 cm^{-1} can be assigned to the stretching of the carbonyls (C=O) of the ester groups. The different peaks observed at 1470, 1397, 1368 cm^{-1} are associated to CH_2 bending mode; peaks at 1243, 1108 and 1045 cm^{-1} can be attributed to C-O-C stretching. Other bands between 1164 cm^{-1} and 1194 cm^{-1} are also associated to C–O and O–C–O stretching, respectively [42].

The spectra of binary PE/PCL blends as function of composition (Figure 1a) were found to be similar to that of neat PCL. The different characteristic bands of PCL are present in the spectra of the blends, and they are independent of PCL concentration.

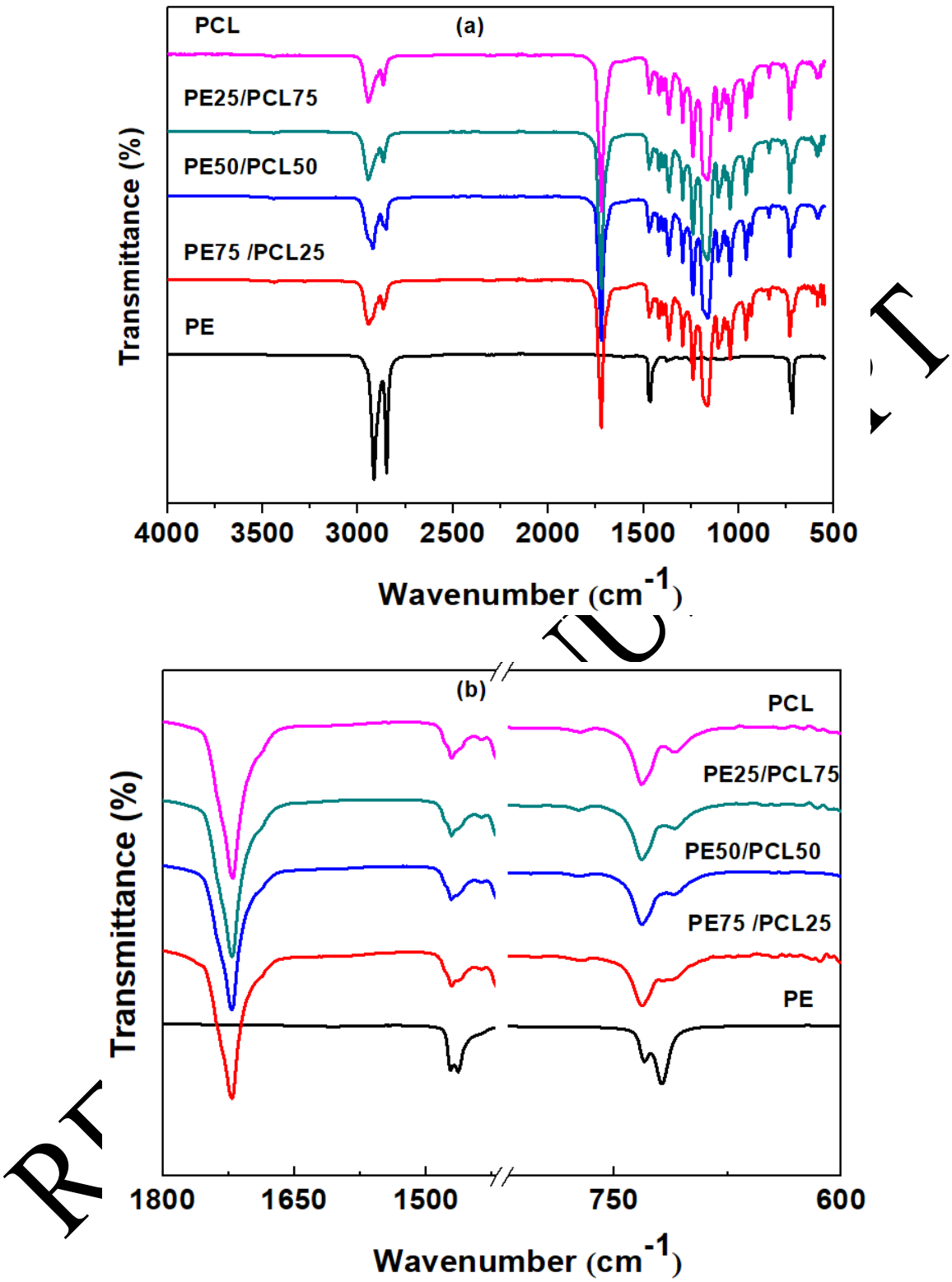

Fig. 1. (a) ATR-FTIR spectra of PE, PCL, and their blends; (b) the same spectra in the wavenumber range between 1800 and 700 cm^{-1}.

Figure 1b represents an enlarged view of Figure 1a between 1650 cm^{-1} and 680 cm^{-1}. The doublet at 1473-1463 cm^{-1}, corresponding to symmetric and asymmetric C-H stretching of

PE, decreases and merges to form a large band for PCL-containing blends. Moreover, the two bands situated around 730 cm^{-1} show inversion of their intensities after incorporation of PCL. These results indicate the presence of certain interactions between PE and PCL chains. Similar results were obtained by Blázquez-Blázquez et al. [43].

The FTIR spectra of EGMA and PE75/PCL25, containing 0, 1, and 5Phr of EGMA, are shown in Figure 2. The EGMA spectrum exhibits absorption bands at 997, 910 and 848 cm^{-1} associated to the epoxy group, a band at 1730 cm^{-1} indicating the presence of a C=O group, as well as the characteristic bands of PE [37,44]. In contrast, peaks from glycidyl groups (EGMA) (997-848 cm^{-1}) are imperceptible in the spectra of PE75/PCL25 with 1 and 5 Phr of EGMA. A new small band appears, corresponding to a hydroxyl group (OH) in the region of 3200 cm^{-1}, indicating a reaction between the epoxy group of EGMA and hydroxyl end groups of PCL [45,46].

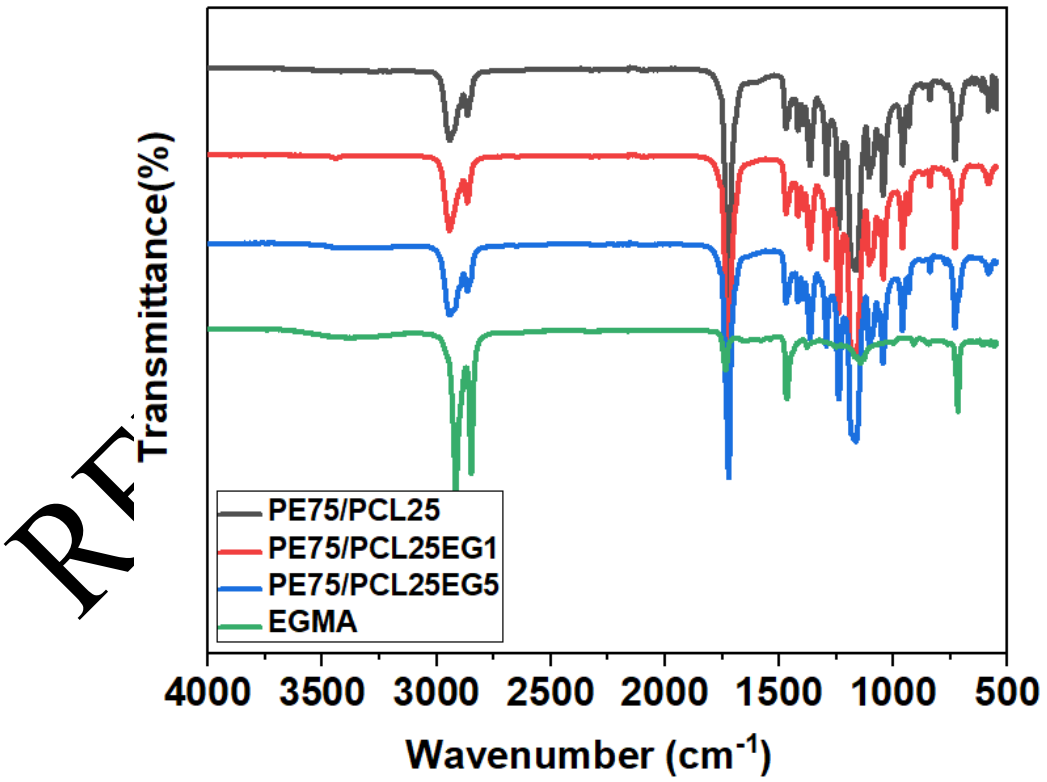

Fig. 2. FTIR spectra of EGMA, PE75/PCL25 compatibilized with 1 and 5Phr of EGMA.

The spectrum of Ox-PE75/PCL25 blend, displayed in Figure 3, presents nearly the same bands compared to those of PE. The changes, taking place on the Ox-PE75/ PCL25 spectrum, are especially situated in the range from 1400 to 700 cm^{-1}. They are associated to CH_2 bending mode and C-O-C stretching. One observes also a reduction of the band at 1720cm^{-1}, and an increase of the doublet at 2944-2865 cm^{-1}. Such findings could reflect the strong activity of pro-oxidants to induce thermo-oxidation processes in PE phase [47–51], which promote generation of peroxyl and /or alkoxyl radicals, formation of carbonyl groups on PE backbone, leading to chain scission, and formation of oxidation products. These processes are extensively described in literature [38].

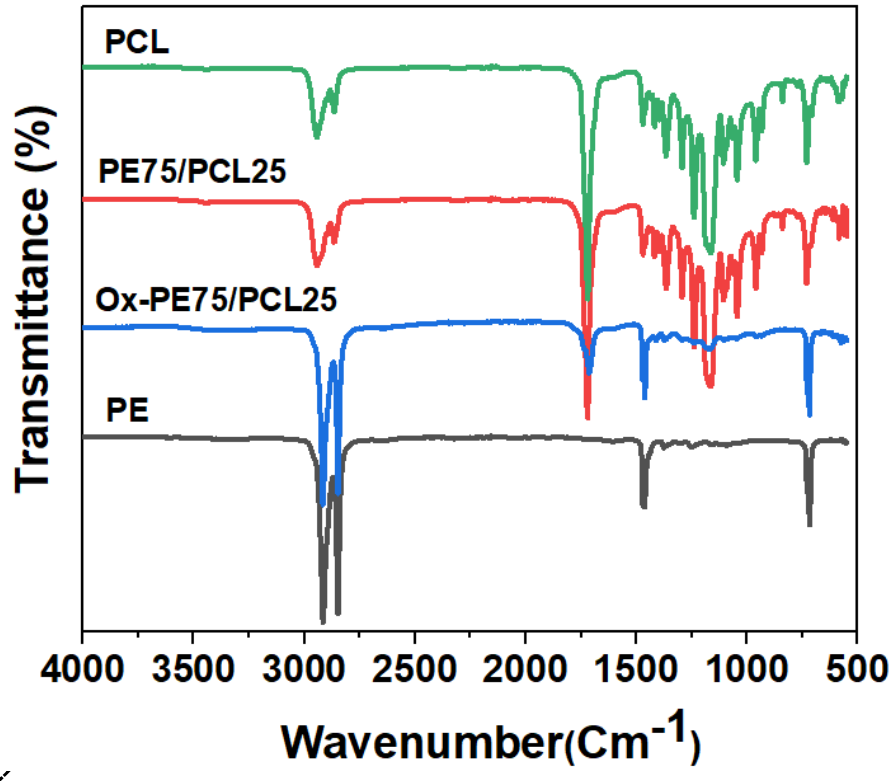

Fig. 3. FTIR spectra of PE, PCL, PE75/PCL25 and Ox-PE75/PCL25.

Furthermore, the oxidation products generated along the chains during shear melt blending of Ox-PE75/PCL25, can create successful interaction with PCL chains. Indeed, the apparent reduction of the band intensity at 1721 cm^{-1} (carbonyl group) (Figure 3) and the disappearance of the bands between 1400 and 700 cm^{-1} may be a significant proof of

interaction between Ox-PE and PCL chains during the melting process, which may result in the formation of new polymer chain arrangements. Following these remarks, an attempt was made to visualize by SEM observations the change of compatibility in these blends.

4.2. Analysis of morphology

SEM micrographs of fractured surfaces of the elaborated materials are displayed in Figure 4. In the case of the PE75/PCL25 blend (Figure 4a), a typical morphology of an immiscible system appears where two separate phases, corresponding to each compound, were observed. They are distributed in the form of a nodular morphology, consisting of a dispersion of spheres (or nodules) of PCL as the minority phase, in the PE matrix as majority phase.

Figure 4b and 4c indicate that, due to the diffusion effect introduced by EGMA chains at the interface; addition of EGMA causes a decrease of the size of PCL particles in the immiscible PE75/PCL25 blend. This effect is more pronounced for 5 Phr EGMA than for 1 phr. It can be deduced that EGMA act synergistically to reduce the particle size of the dispersed phase. A relatively uniform particle distribution within the matrix was observed. The same effect has been described in literature for other polymer systems [52–54].

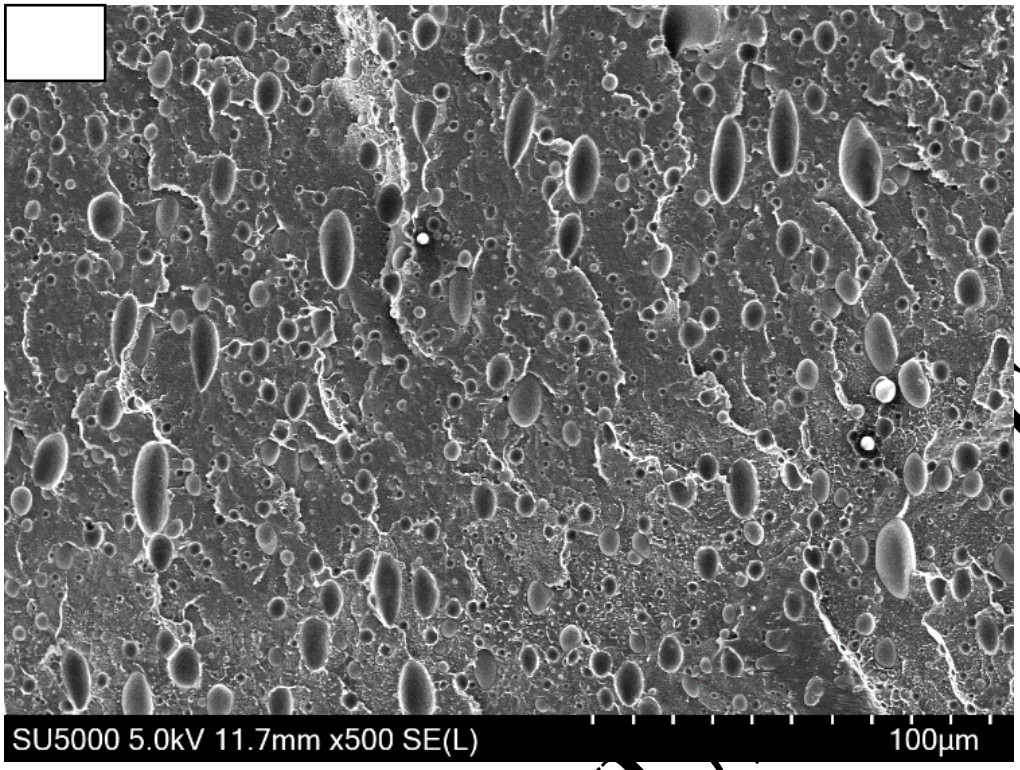
SU5000 5.0kV 11.7mm x500 SE(L)
100µm

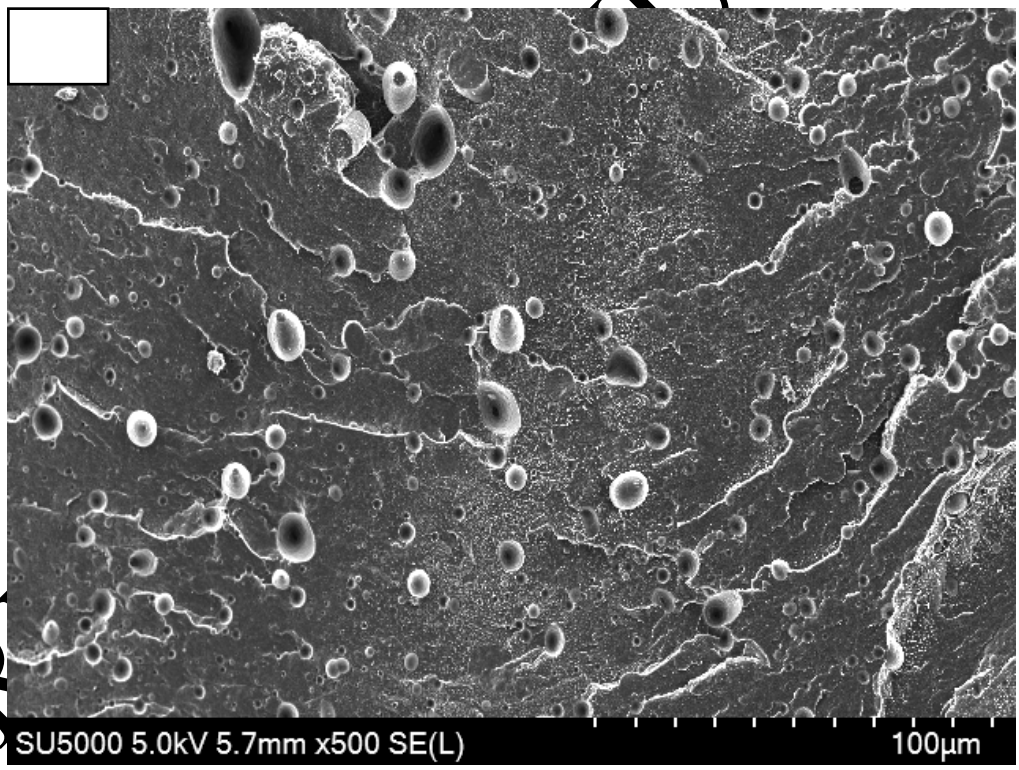
SU5000 5.0kV 5.7mm x500 SE(L)
100µm

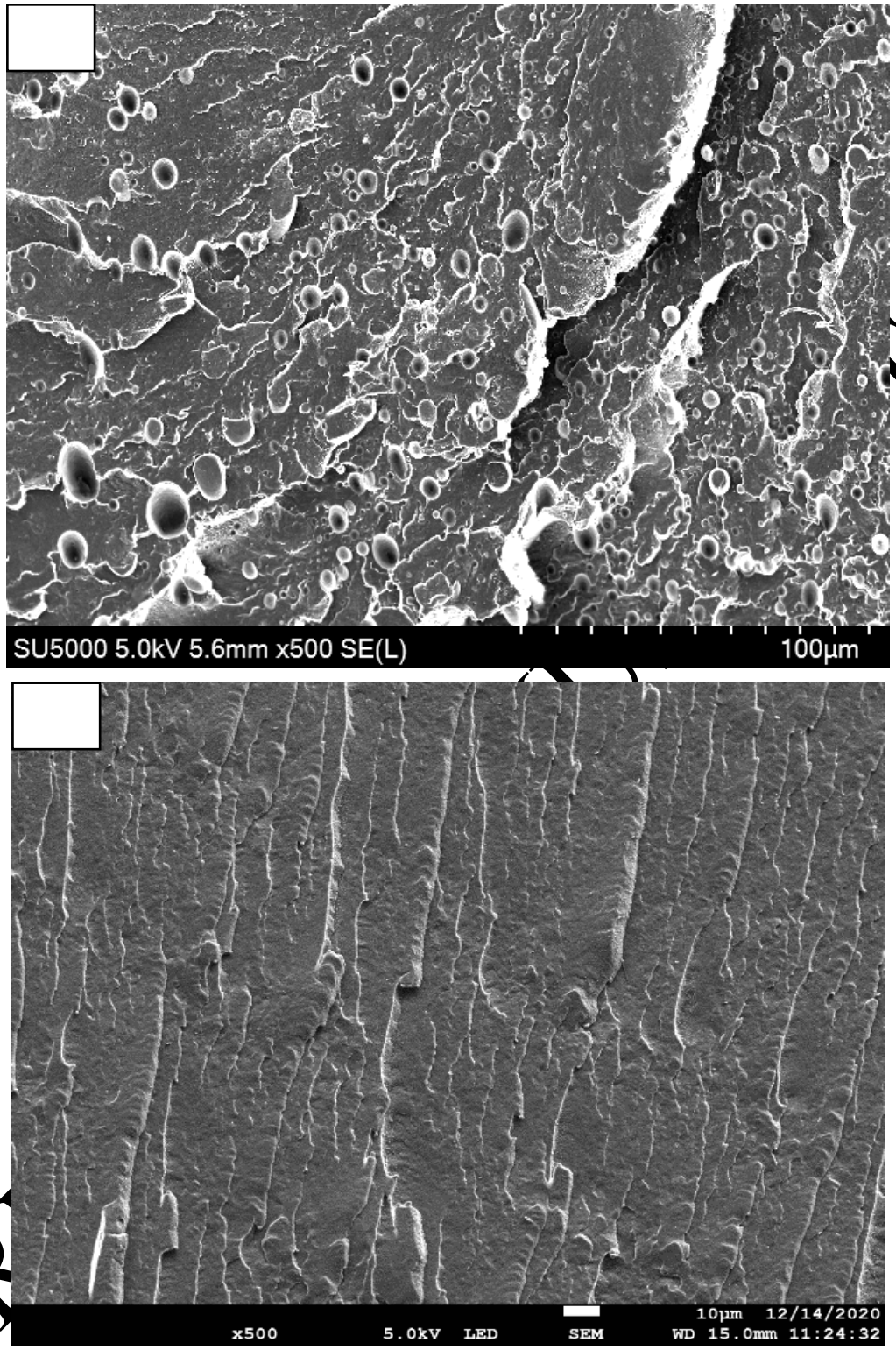

Fig. 4. SEM micrographs of the fracture surface of (a) PE75/PCL25, (c) PE75/PCL25EG1, (d) PE75/PCL25EG5 and (d) Ox-PE75/PCL25.

4.3. Differential Scanning Calorimetry

Figures 5 and 6 illustrate thermograms corresponding to the second heating and cooling cycles of PE, PCL, binary PE/PCL blends, and tertiary PE75/PCL25/EGMA systems. The thermograms of PE100 show an endothermic peak at 106°C and an exothermic peak at 101°C related, respectively, to melting and crystallization occurring in the crystalline phase of PE. The DSC curve of PCL exhibits a melting temperature at around 55°C and a crystallization temperature at 35°C. Furthermore, the thermograms of PE/PCL blends present exo- and endothermic peaks corresponding to fusion and crystallization of the homopolymers. In the heating cycle (Figure 5a), the melting temperature (Tm) of PE increases smoothly with incorporation of PCL from 106°C (PE75/PCL25) to 111°C (PE25/PCL75). The cooling cycles of PE/PCL blends present two crystallization peaks, the first one in the range from -101°C to -104°C, and the second one between -31°C and -34°C, which can be attributed to PE and PCL, respectively. The thermal data of all samples are illustrated in Table 2.

A small increase of the crystallization temperature (Tc) of PE as well as a decrease of Tc of PCL was observed with increasing PCL content in the binary PE/PCL blends. This is due to the fact that PE crystallizes at higher temperatures than PCL. As a consequence, PCL chains could undergo confinement effects into small volumes of lamellar crystallized PE [55]. The degree of crystallinity (Xc) of both PE and PCL phases in the blends shows slightly decreased values compared to those of the neat homopolymers, thus suggesting a certain compatibility between PCL and PE chains. Different explanations have been proposed in literature to understand this behavior [56].

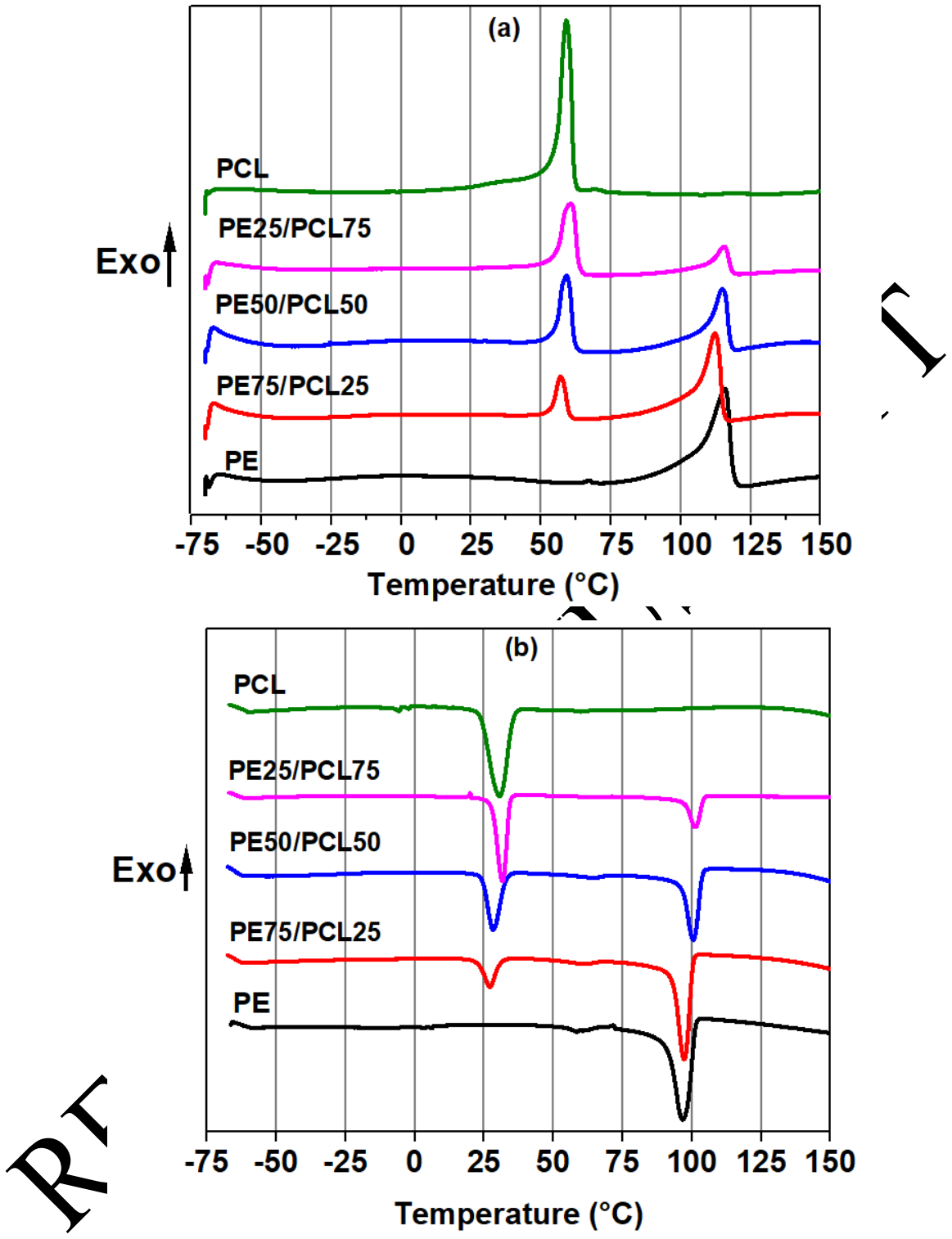

Fig. 5. Thermograms of (a) second heating, (b) cooling curves recorded at a scan rate of 10°C/min for PE, PCL and PE/PCL binary blends.

Table 2

Thermal properties of neat LDPE, PCL and their blends obtained from DSC thermograms.

Sample	Heating cycle				Cooling cycle				X_C (%)	
	PE		PCL		PE		PCL		PE	PCL
	Tm ±0.1(°C)	ΔH_m(J/g)	Tm±0.1(°C)	ΔH_m(J/g)	Tc±0.1(°C)	ΔH_c (J/g)	Tc ±0.1(°C)	ΔH_c(J/g)		
PE	106	64.99	/		101	-64.32	/	/	22.17	/
PE75/PCL25	107	47.78	54	11.56	100	-47.41	31	-13.53	21.73	33.14
PE50/PCL50	109	30.35	55	25.51	103	-30.23	33	-27.57	20.70	36.57
PE25/PCL75	111	12.11	56	34.86	104	-13.59	34	-39.11	16.52	33.31
PCL	/	/	55	54.14	/	/	35	-55.72	/	38.81
PE75/PCL25EG1	108	47.80	54	11.91	104	-56.82	28	-18.47	21.47	34.15
PE75/PCL25EG5	108	41.23	53	11.38	104	-52.71	23	-9.31	18.75	34.06
Ox-PE75/PCL25	109	39.93	55	7.61	110	-35.48	33	-8.49	18.15	21.82

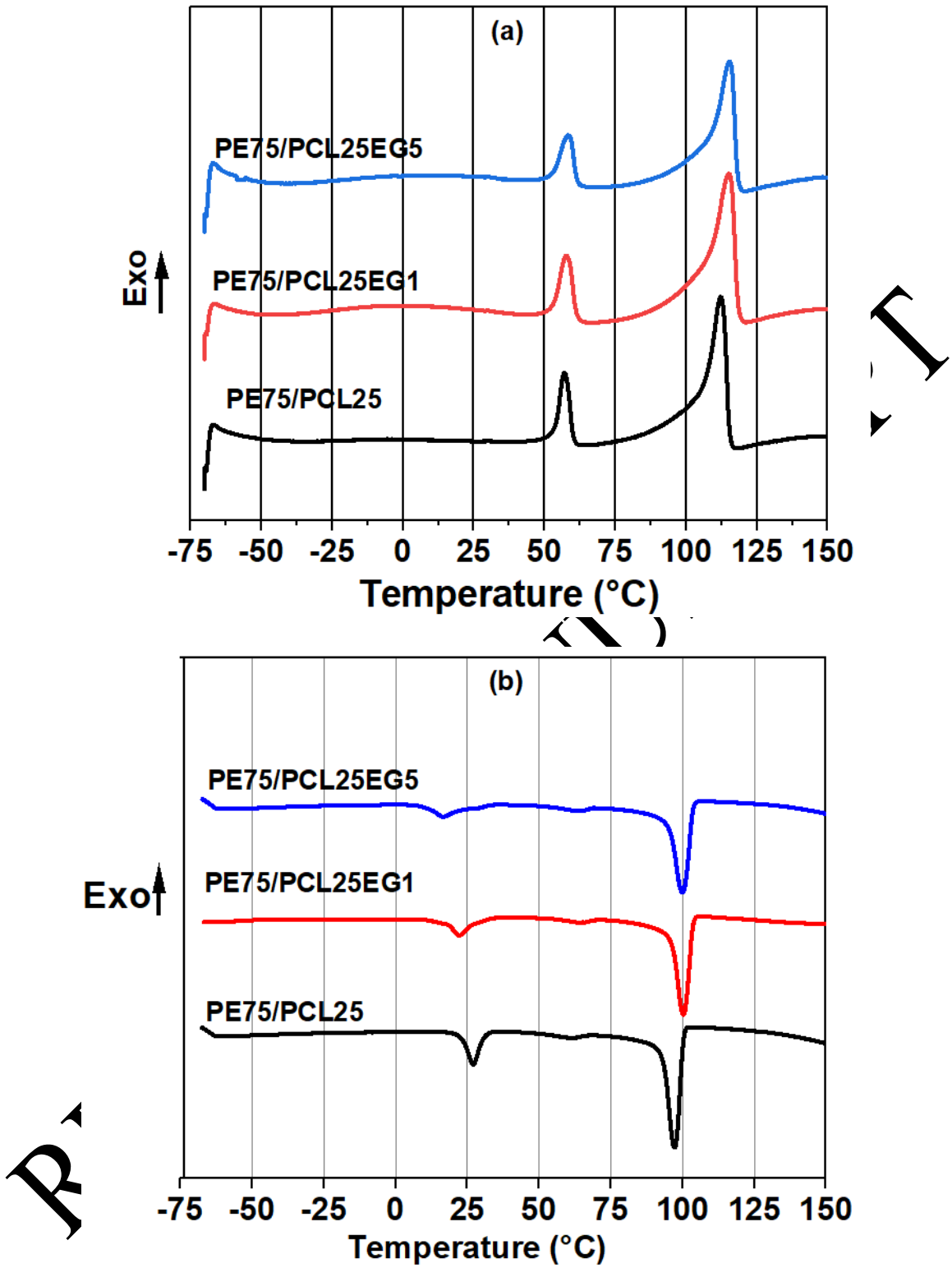

Fig. 6. DSC thermograms of (a) heating and (b) cooling ramps for PE75/PCL25 blends in the presence of 1 and 5 Phr of EGMA.

The thermograms of ternary blends composed of PE75/PCL25 and EGMA are presented in Figure 6. The displayed thermograms exhibit similar thermal events compared to those of

PE/PCL blends, with exception of a change in intensity of PCL peaks. Adding EGMA leads to an increase of melting and crystallization temperatures of PE and a decrease of the crystallization temperature of PCL (Table 2). The Xc values of PE75/PCL25/EG1 were found to be similar compared to PE75/PCL25. However, at 5 Phr of EGMA, Xc (PE) strongly decreased, which could be attributed to the interface formation by the reaction between the epoxy ring of EGMA and hydroxyl end groups of PCL during melt-blending. This interface contributed to modify interfacial adhesion between PE and PCL, which is in good agreement with results obtained in the literature [57].

Figures 7a and 7b represent DSC thermograms of heating and cooling ramps for PE75/PCL25 and Ox-PE75/PCL25 blends, respectively. The results from thermal data analysis were gathered in Table 2. The thermogram of Ox-PE/PCL (Figure 7a) reveals similar thermal events compared to PE/PCL, accompanied with a small increase of the melting temperature of Ox-PE. During the cooling ramps a shift of the crystallization temperature of Ox-PE and PCL to higher temperatures was observed together with a change of the shape of the crystallization curves of PE. Changes of enthalpy and temperature values for PE and PCL in the Ox-PE/PCL system can be explained by the reorganization of polymers chains and formation of new crystalline phases after incorporating pro-oxidants in the PE phase.

The crystallinity degrees of PE and PCL phases in the blend decreased from 21.7% in PE/PCL to 18.2% in Ox-PE/PCL and from 33.1% in PE/PCL to 21.8% in Ox-PE/PCL, respectively. This reduction of the crystallinity in the PE phase can be explained by the incorporation of pro-oxidants in the PE matrix, which initiate the oxidation process in the polymeric chain and lead to the formation of polar groups [27,58–60].

The decrease of crystallinity of the PCL phase in Ox-PE/PCL system is related to the sample morphology. Indeed, the decrease of the size of the dispersed phase in the Ox-PE/PCL blend, compared to the PE/PCL system (Figure 4), provokes a reduction of the crystallinity of the

PCL phase. Similar results were reported by several authors for other polymer systems [61].

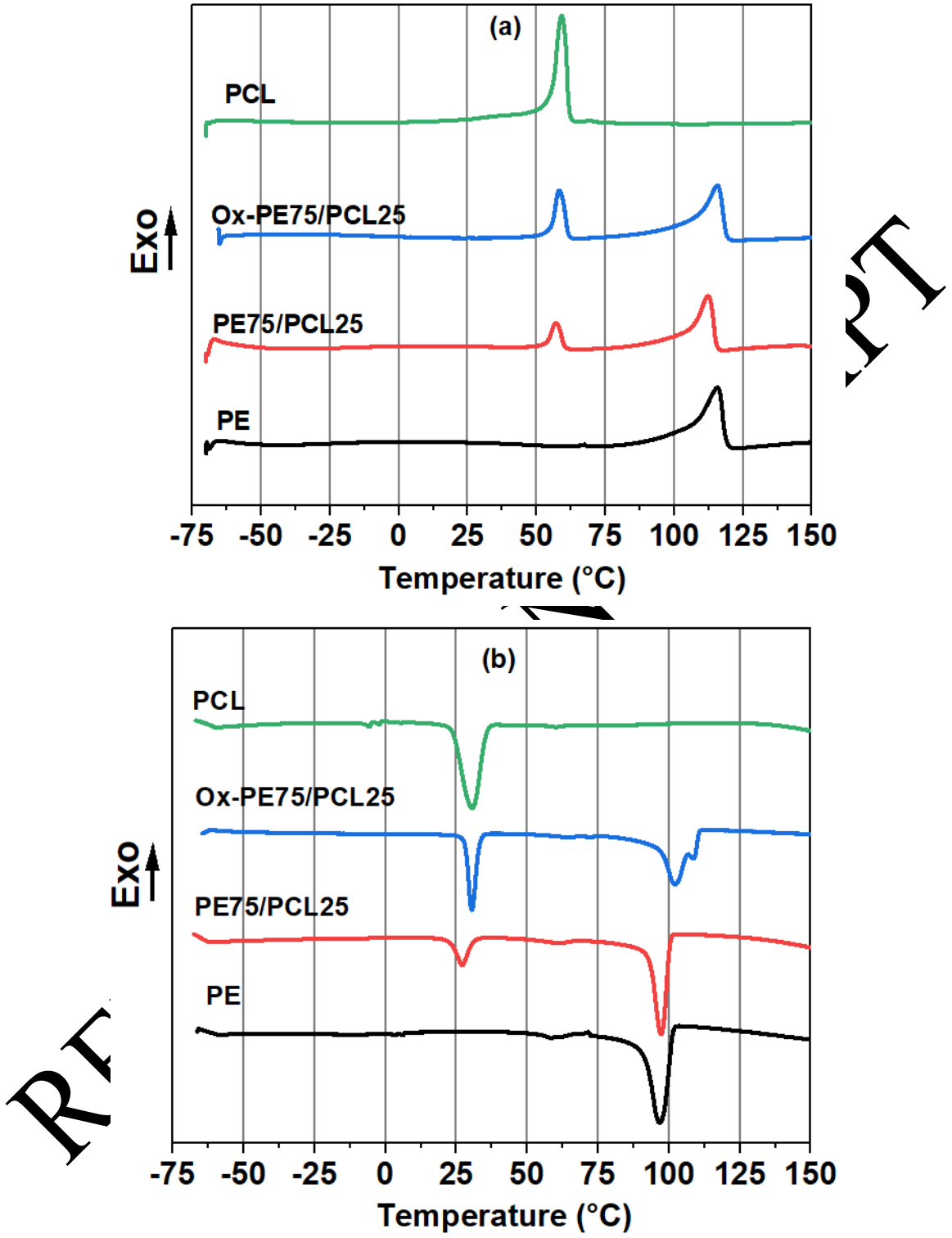

Fig. 7. DSC thermograms of (a) heating and (b) cooling ramps for PE75/PCL25 and Ox-PE75/PCL25 blends.

4.4. Thermogravimetric analysis

The results of TGA analysis of neat homopolymers and the different blends are illustrated in Figure 8, and the important degradation temperatures are presented in Table 3. T_{onset} is the temperature corresponding to 5% of mass loss, T_f corresponds to the temperature of the end of degradation related to a mass loss of 95%, and T_{dmax} stands for the temperature corresponding to the maximum of mass loss. TGA curves of pure PCL and PE showed single decomposition steps with T_{dmax} of 409°C and 496°C, respectively (see Figure 8b). PE starts degradation at around T_{onset}= 411°C and finishes at around T_f= 496°C, whereas PCL begins the degradation process at T_{onset} =367°C, ending at T_f= 448°C. Figure 8a as well as Table 3 indicates that PE is thermally more stable than PCL, since it degrades at higher temperatures.

Table 3
TGA data of PE, PCL and their blends.

Samples	T_{onset}(°C)	T_{dmax1}(°C)	T_{dmax2}(°C)	T_f(°C)
PE	411	/	469	496
PCL	367	409		448
PE75/PCL25	390	409	475	487
PE75/PCL25EG1	382	404	462	484
PE75/PCL25EG5	387	407	469	489
Ox-PE75/PCL25	376	398	478	490

The PE75/PCL25 blends show an intermediate behavior between PE and PCL (Figure 8a) with a decomposition temperature comprised between those of PE and PCL. Indeed, PCL decomposes at a lower temperature than PE. The PE75/PCL25 binary blend exhibits a two-state decomposition process which can be seen in the thermograms where two main peaks appeared at 409°C and 475°C, which can be attributed to the decomposition processes of PCL and PE, respectively.

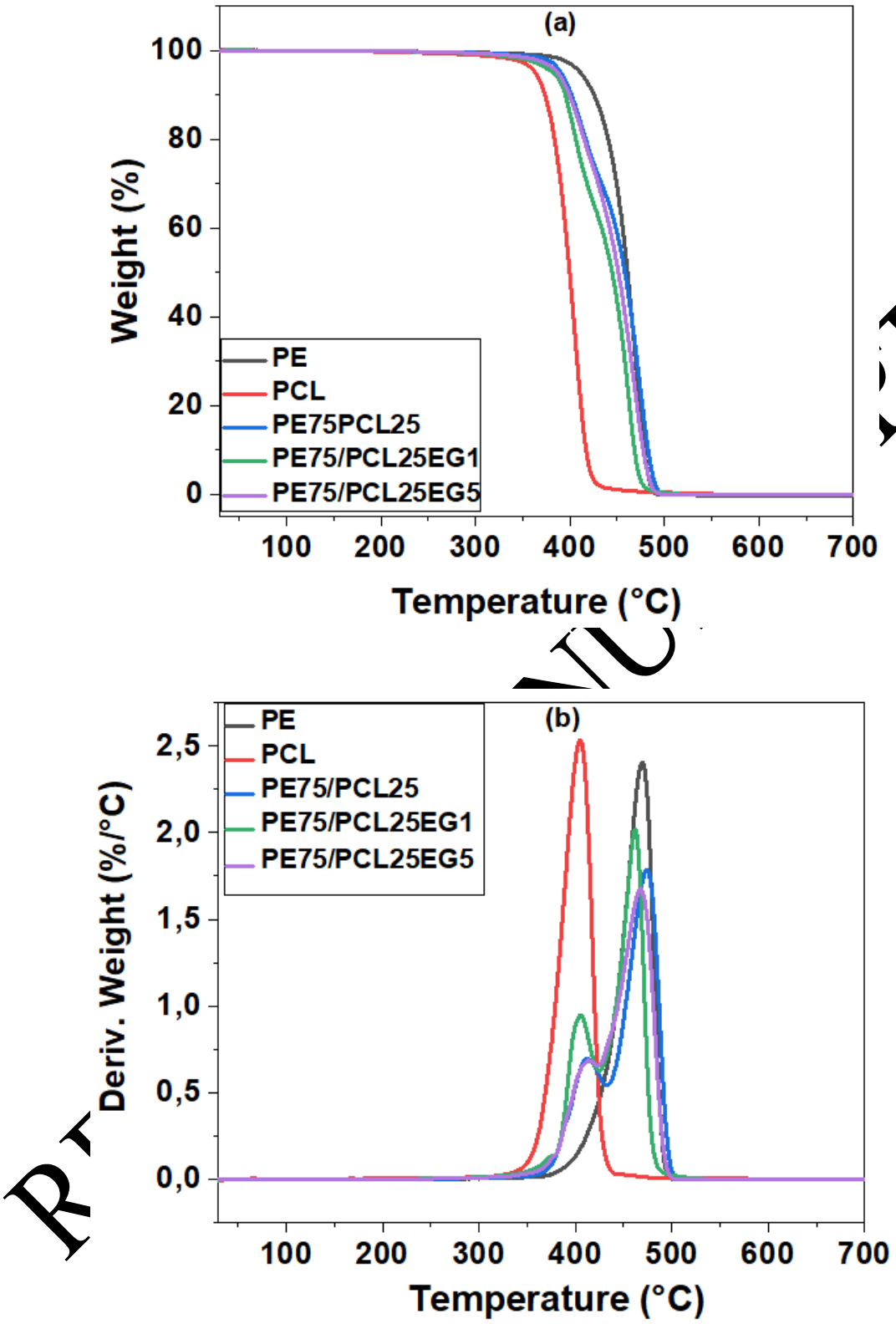

Fig. 8. a) TGA and b) DTA curves of neat homopolymers and their blends.

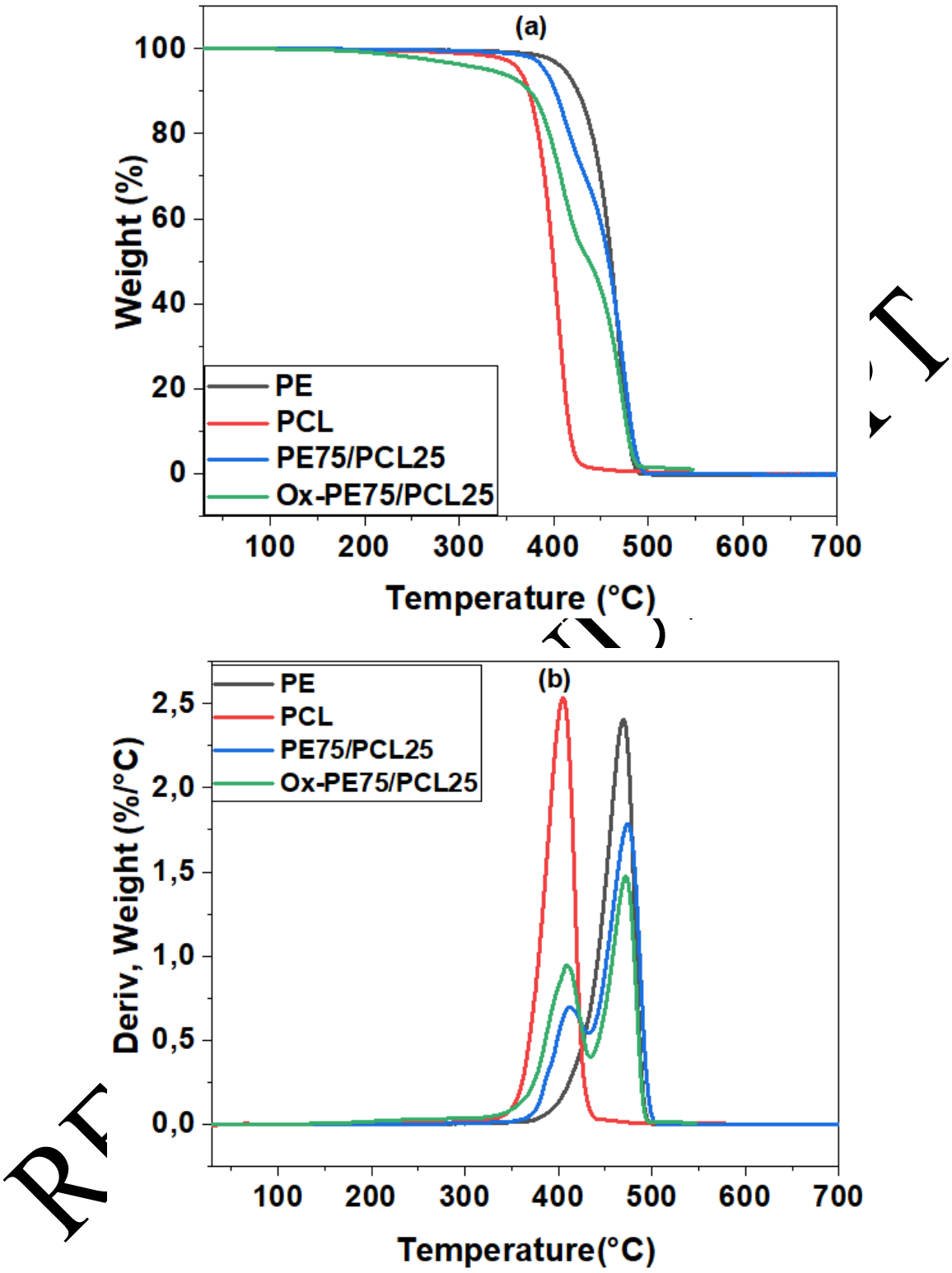

Fig. 9. a) TGA and b) DTA curves of PE75/PCL25 and Ox-PE75/PCL25.

Similarly, two decomposition states were also observed when EGMA was incorporated into the PE75/PCL25 blend (Figure 8), yielding only small changes in T_{onset} and T_f compared to PE75/PCL25. This is probably due to enhanced interaction between the epoxy group of EGMA and the hydroxyl group of PCL.

However, in the case of the Ox-PE75/PCL25 blend, Figure 9a, b and Table 3 show a reduction of T_{onset} of about 20°C compared to the other systems (PE, PCL, PE75/PCL25). This may be attributed to the catalyst effect of the pro-oxidant and its efficiency to accelerate degradation process of PE [6].

These modifications, occurring in the PE matrix, promote the Ox-PE75/PCL25 system to begin thermal degradation at lower temperatures than the other blends, resulting in a decrease of thermal stability.

Conclusions

In this paper, several approaches have been developed to enhance compatibility between PE and PCL, which can be a solution for the treatment of end-of-life PE waste.

A series of PE/PCL blends were prepared and examined. FTIR and DSC results showed certain interaction between PE and PCL chains. EGMA copolymer was used in an attempt to increase compatibility within PE/PCL blends. Morphology analysis demonstrate that the size of the dispersed phase was slightly decreased in the presence of EGMA which can be explained by the reaction between hydroxyl end groups of PCL and epoxy group of EGMA at the interface. However no significant change in thermal degradation was achieved.

Structure modification of PE was realized by thermo-oxidation in the presence of pro-oxidants. The crucial point consists in the fact that this thermo-oxidation was performed before PE was mixed with PCL. This is the principal reason for the creation of interaction and thus enhancement of compatibility, yielding a decrease of crystallinity and thermal stability.

The trick of adding pro-oxidants to the PE matrix before blending with PCL ensured that thermo-oxidation took place on the PE chain. This method of elaboration allows developing a new strategy to obtain compatibility in melt blending with PCL or other biodegradable polymers, meeting thus the challenge of preventing pollution in the environment caused by end-of-life PE.

Acknowledgements

The first author (H.B.) received a scholarship under the Profas B+ PhD-program between Algeria and France. Our thanks therefore go first of all to the various actors who participated in the implementation of this program. The authors gratefully acknowledge the support of the Algerian Ministry of Higher Education and Scientific Research (MESRS), the General Directorate of Scientific Research and Technological Development (DGRSDT) of Algeria, the University of Sétif/Algeria, the French Ministry of Higher Education and Research (MENESR), the CNRS, and the University and the CROUS of Lille/France.

References

[1] K.R. Vanapalli, J. Bhattacharya, B. Samal, S. Chandra, I. Medha, B.K. Dubey, Single-use LDPE + Eucalyptus biomass char composite produced from co-pyrolysis has the properties to improve the soil quality, Process Saf. Environ. Prot. 149 (2021) 185–198. https://doi.org/10.1016/j.psep.2020.10.051.

[2] A. Vázquez-Morillas, M. Beltrán-Villavicencio, J.C. Alvarez-Zeferino, M.H. Osada-Velázquez, A. Moreno, L. Martínez, J.M. Yañez, Biodegradation and Ecotoxicity of Polyethylene Films Containing Pro-Oxidant Additive, J. Polym. Environ. 24 (2016) 221–229. https://doi.org/10.1007/s10924-016-0765-8.

[3] M. Taghavi, I.A. Udugama, W.Q. Zhuang, S. Baroutian, Challenges in biodegradation of non-degradable thermoplastic waste: From environmental impact to operational readiness, Biotechnol. Adv. 49 (2021) 107731. https://doi.org/10.1016/j.biotechadv.2021.107731.

[4] M.R. Johansen, T.B. Christensen, T.M. Ramos, K. Syberg, A review of the plastic value chain from a circular economy perspective, J. Environ. Manage. 302 (2022) 113975. https://doi.org/10.1016/j.jenvman.2021.113975.

[5] L. Ren, L. Men, Z. Zhang, F. Guan, J. Tian, B. Wang, J. Wang, Y. Zhang, W. Zhang, Biodegradation of polyethylene by enterobacter sp. D1 from the guts ofwax moth galleria mellonella, Int. J. Environ. Res. Public Health. 16 (2019) 1941.

https://doi.org/10.3390/ijerph16111941.
[6] G. Madhu, H. Bhunia, P.K. Bajpai, G.B. Nando, Physico-mechanical properties and biodegradation of oxo-degradable HDPE/PLA blends, Polym. Sci. - Ser. A. 58 (2016) 57–75. https://doi.org/10.1134/S0965545X16010077.
[7] S.M. Al-Salem, A. Al-Hazza'a, H.J. Karam, M.H. Al-Wadi, A.T. Al-Dhafeeri, A.A. Al-Rowaih, Insights into the evaluation of the abiotic and biotic degradation rate of commercial pro-oxidant filled polyethylene (PE) thin films, J. Environ. Manage. 250 (2019) 109475. https://doi.org/10.1016/j.jenvman.2019.109475.
[8] C.M. Plummer, L. Li, Y. Chen, The post-modification of polyolefins with emerging synthetic methods, Polym. Chem. 11 (2020) 6862–6872. https://doi.org/10.1039/d0py01279c.
[9] T.M. Karlsson, M. Hassellöv, I. Jakubowicz, Influence of thermooxidative degradation on the in situ fate of polyethylene in temperate coastal waters, Mar. Pollut. Bull. 135 (2018) 187–194. https://doi.org/10.1016/j.marpolbul.2018.07.015.
[10] Z. Oksiuta, M. Jalbrzykowski, J. Mystkowska, E. Romanczuk, T. Osiecki, Mechanical and thermal properties of polylactide (PLA) composites modified with Mg, Fe, and polyethylene (PE) additives, Polymers (Basel). 12 (2020) 2939. https://doi.org/10.3390/polym12122939.
[11] E.B. Bezerra, D.C. de França, D.D. de S. Morais, I.D. dos S. Silva, D.D. Siqueira, E.M. Araújo, R.M.R. Wellen, Compatibility and characterization of Bio-PE/PCL blends, Polímeros. 29 (2019) e2019022. https://doi.org/10.1590/0104-1428.02518.
[12] K. Hamad, M. Kaseem, Y.G. Ko, F. Deri, Biodegradable polymer blends and composites: An overview, Polym. Sci. Ser. A. 56 (2014) 812–829. https://doi.org/10.1134/S0965545X14060054.
[13] S. Djellali, N. Haddaoui, T. Sadoun, A. Bergeret, Y. Grohens, Structural, morphological and mechanical characteristics of polyethylene, poly(lactic acid) and poly(ethylene-co-glycidyl methacrylate) blends, Iran. Polym. J. 22 (2013) 245–257. https://doi.org/10.1007/s13726-013-0126-6.
[14] S. Djellali, T. Sadoun, N. Haddaoui, A. Bergeret, Viscosity and viscoelasticity measurements of low density polyethylene/poly(lactic acid) blends, Polym. Bull. 72 (2015) 1177–1195. https://doi.org/10.1007/s00289-015-1331-6.
[15] N. Medjdoub, M. Guessoum, M. Fois, Viscoelastic, thermal and environmental characteristics of poly(lactic acid), linear low-density polyethylene and low-density polyethylene ternary blends and composites, J. Adhes. Sci. Technol. 31 (2017) 787–805. https://doi.org/10.1080/01694243.2016.1232547.
[16] M. V. Podzorova, Y. V. Tertyshnaya, Degradation of Polylactide—Polyethylene Binary Blends in Soil, Russ. J. Appl. Chem. 92 (2019) 767–774. https://doi.org/10.1134/S1070427219060065.
[17] M.S. Khan, P.P. Dhavan, D. Ratna, S.S. Sonawane, N.G. Shimpi, LDPE:PLA and LDPE:PLA:OMMT polymer composites: Preparation, characterization, and its biodegradation using Bacillus species isolated from dumping yard, Polym. Adv. Technol. 32 (2021) 3724–3739. https://doi.org/10.1002/pat.5392.
[18] B.M. Lekube, C. Burgstaller, Study of mechanical and rheological properties, morphology, and miscibility in polylactid acid blends with thermoplastic polymers, J. Appl. Polym. Sci. 139 (2022) 51662. https://doi.org/10.1002/app.51662.
[19] G.A.D. Burlein, M.C.G. Rocha, Mechanical and morphological properties of LDPE/ PHB blends filled with castor oil pressed cake, Mater. Res. 17 (2013) 97–105. https://doi.org/10.1590/S1516-14392013005000196.
[20] T. Sadik, V. Massardier, F. Becquart, M. Taha, Polyolefins/Poly(3-hydroxybutyrate- co -hydroxyvalerate) blends compatibilization: Morphology, rheological, and mechanical

properties, J. Appl. Polym. Sci. 127 (2013) 1148–1156. https://doi.org/10.1002/app.37957.
[21] D.C. França, D.D. Morais, E.B. Bezerra, E.M. Araújo, R.M. Ramos Wellen, Photodegradation mechanisms on poly(ε-caprolactone) (PCL), Mater. Res. 21 (2018) e20170837. https://doi.org/10.1590/1980-5373-MR-2017-0837.
[22] S. Salehi, T. Bahners, J.S. Gutmann, S.L. Gao, E. Mäder, T.A. Fuchsluger, Characterization of structural, mechanical and nano-mechanical properties of electrospun PGS/PCL fibers, RSC Adv. 4 (2014) 16951–16957. https://doi.org/10.1039/c4ra01237b.
[23] M. Nevoralová, M. Koutný, A. Ujčić, Z. Starý, J. Šerá, H. Vlková, M. Šlouf, I. Fortelný, Z. Kruliš, Structure Characterization and Biodegradation Rate of Poly(ε-caprolactone)/Starch Blends, Front. Mater. 7 (2020) 141. https://doi.org/10.3389/fmats.2020.00141.
[24] J. juan Su, F. Zhu, Y. Meng, J. Han, K. Wang, Q. Fu, Significant toughness improvement in iPP/PLLA/EGMA blend by introducing dicumyl peroxide as the morphology governor, Colloid Polym. Sci. 296 (2018) 31–39. https://doi.org/10.1007/s00396-017-4225-3.
[25] F. Bensaad, N. Belhaneche-Bensemra, Effects of calcium stearate as pro-oxidant agent on the natural aging of polypropylene, J. Polym. Eng. 38 (2018) 715–721. https://doi.org/10.1515/polyeng-2017-0391.
[26] K. Glowik-Lazarczyk, S. Jurczyk, B. Chmielnicki, J. Konieczny, K. Labisz, Influence of oxo-degradable pe recyclate addition on the degradation of commercial low density polyethylene (PE-LD), J. Environ. Prot. Ecol. 18 (2017) 947–961.
[27] D.K. Mandal, H. Bhunia, P.K. Bajpai, Thermal degradation kinetics of oxo-degradable PP/PLA blends, J. Polym. Eng. 39 (2019) 58–67. https://doi.org/10.1515/polyeng-2018-0073.
[28] M. Subramaniam, S. Sharma, A. Gupta, N. Abdullah, Enhanced degradation properties of polypropylene integrated with iron and cobalt stearates and its synthetic application, J. Appl. Polym. Sci. 135 (2018) 46028. https://doi.org/10.1002/app.46028.
[29] P.K. Roy, P. Surekha, R. Raman, C. Rajagopal, Investigating the role of metal oxidation state on the degradation behaviour of LDPE, Polym. Degrad. Stab. 94 (2009) 1033–1039. https://doi.org/10.1016/j.polymdegradstab.2009.04.025.
[30] B. Suresh, S. Maruthamuthu, A. Khare, N. Palanisamy, Influence of thermal oxidation on surface and thermo-mechanical properties of polyethylene, J. Polym. Res. 18 (2011) 2175–2184. https://doi.org/10.1007/s10965-011-9628-0.
[31] C. Abrusci, J.L. Pablos, I. Marín, E. Espí, T. Corrales, F. Catalina, Comparative effect of metal stearates as pro-oxidant additives on bacterial biodegradation of thermal- and photo-degraded low density polyethylene mulching fi lms, Int. Biodeterior. Biodegradation. 83 (2013) 25–32. https://doi.org/10.1016/j.ibiod.2013.04.002.
[32] J.L. Pablos, C. Abrusci, I. Marín, J. López-marín, F. Catalina, E. Espí, T. Corrales, Photodegradation of polyethylenes□: Comparative effect of Fe and Ca-stearates as pro-oxidant additives, Polym. Degrad. Stab. 95 (2010) 2057–2064. https://doi.org/10.1016/j.polymdegradstab.2010.07.003.
[33] L. Yu, X. Liu, E. Petinakis, S. Bateman, P. Sangwan, A. Ammala, K. Dean, S. Wong-holmes, Q. Yuan, C.K. Siew, F. Samsudin, Z. Ahamid, Enhancement of Pro-Degradant Performance in Polyethylene / Starch Blends as a Function of Distribution, J. Appl. Polym. Sci. 128 (2013) 591–596. https://doi.org/10.1002/app.38229.
[34] S. Fontanella, S. Bonhomme, J. Brusson, S. Pitteri, G. Samuel, G. Pichon, J. Lacoste, D. Fromageot, J. Lemaire, A. Delort, Comparison of biodegradability of various polypropylene fi lms containing pro-oxidant additives based on Mn , Mn / Fe or Co,

Polym. Degrad. Stab. 98 (2013) 875–884. https://doi.org/10.1016/j.polymdegradstab.2013.01.002.
[35] S. Sable, S. Ahuja, H. Bhunia, Studies on Biodegradability of Cobalt Stearate Filled Polypropylene After Abiotic Treatment, J. Polym. Environ. 28 (2020) 2236–2252. https://doi.org/10.1007/s10924-020-01762-3.
[36] A. Gharehdashli, S. Mortazavi, Photodegradation of low-density polyethylene with prooxidant and photocatalyst, J. Appl. Polym. Sci. 137 (2020) 48979. https://doi.org/10.1002/app.48979.
[37] F.-C. Pai, H.-H. Chu, S.-M. Lai, Reactive compatibilization of poly(lactic acid)/polyethylene octene copolymer blends with ethylene-glycidyl methacrylate copolymer, J. Polym. Eng. 31 (2011) 463–471. https://doi.org/10.1515/POLYENG.2011.091.
[38] S. Chatterjee, B. Roy, D. Roy, R. Banerjee, Enzyme-mediated biodegradation of heat treated commercial polyethylene by Staphylococcal species, Polym. Degrad. Stab. 95 (2010) 195–200. https://doi.org/10.1016/j.polymdegradstab.2009.11.025.
[39] N.M. Moo-Tun, A. Valadez-González, J.A. Uribe-Calderon, Thermo-oxidative aging of low density polyethylene blown films in presence of cellulose nanocrystals and a pro-oxidant additive, Polym. Bull. 75 (2018) 3149–3169. https://doi.org/10.1007/s00289-017-2204-y.
[40] X. Jing, H.Y. Mi, H.X. Huang, L.S. Turng, Shape memory thermoplastic polyurethane (TPU)/poly(ε-caprolactone) (PCL) blends as self-knotting sutures, J. Mech. Behav. Biomed. Mater. 64 (2016) 94–103. https://doi.org/10.1016/j.jmbbm.2016.07.023.
[41] J. V. Gulmine, P.R. Janissek, H.M. Heise, L. Akcelrud, Polyethylene characterization by FTIR, Polym. Test. 21 (2002) 557–563. https://doi.org/10.1016/S0142-9418(01)00124-6.
[42] V. Fakhri, M. Monem, G. Mir Mohamad Sadeghi, H.A. Khonakdar, V. Goodarzi, N. Karimpour-Motlagh, Impact of poly(ε-caprolactone) on the thermal, dynamic-mechanical and crystallization behavior of polyvinylidene fluoride/poly(ε-caprolactone) blends in the presence of KI-6 mesoporous particles, Polym. Adv. Technol. 32 (2021) 4424–4439. https://doi.org/10.1002/pat.5444.
[43] E. Blázquez-Blázquez, E. Pérez, V. Lorenzo, M.L. Cerrada, Crystalline Characteristics and Their Influence in the Mechanical Performance in Poly(ε-Caprolactone) / High Density Polyethylene Blends, Polymers (Basel). 11 (2019) 1874. https://doi.org/10.3390/polym11111874.
[44] W. Loyens, G. Groeninckx, Phase morphology development in reactively compatibilised polyethylene terephthalate/elastomer blends, Macromol. Chem. Phys. 203 (2002) 1702–1714. https://doi.org/10.1002/1521-3935(200207)203:10/11<1702::AID-MACP1702>3.0.CO;2-6.
[45] W.A. do Nascimento, P. Agrawal, T.J.A. de Mélo, Effect of copolymers containing glycidyl methacrylate functional groups on the rheological, mechanical, and morphological properties of poly(ethylene terephthalate), Polym. Eng. Sci. 59 (2019) 683–693. https://doi.org/10.1002/pen.24982.
[46] Y. Cui, H. Zhou, D. Yin, H. Zhou, X. Wang, An innovative strategy to regulate bimodal cellular structure in chain extended poly(butylene adipate□ co □terephthalate) foams, J. Vinyl Addit. Technol. 27 (2021) 319–331. https://doi.org/10.1002/vnl.21805.
[47] R.D. Maalihan, B.B. Pajarito, Effect of colorant, thickness, and pro-oxidant loading on degradation of low-density polyethylene films during thermal aging, J. Plast. Film Sheeting. 32 (2016) 124–139. https://doi.org/10.1177/8756087915590276.
[48] A. Benítez, J.J. Sánchez, M.L. Arnal, A.J. Müller, O. Rodríguez, G. Morales, Abiotic

degradation of LDPE and LLDPE formulated with a pro-oxidant additive, Polym. Degrad. Stab. 98 (2013) 490–501. https://doi.org/10.1016/j.polymdegradstab.2012.12.011.
[49] T.A. Nguyen, Ø.W. Gregersen, F. Männle, Thermal oxidation of polyolefins by mild pro-oxidant additives based on iron carboxylates and lipophilic amines: Degradability in the absence of light and effect on the adhesion to paperboard, Polymers (Basel). 7 (2015) 1522–1540. https://doi.org/10.3390/polym7081468.
[50] X. Liu, C. Gao, P. Sangwan, L. Yu, Z. Tong, Accelerating the degradation of polyolefins through additives and blending, J. Appl. Polym. Sci. 131 (2014) 9001–9015. https://doi.org/10.1002/app.40750.
[51] B. Suresh, S. Maruthamuthu, A. Khare, N. Palanisamy, V.S. Muralidharan, R. Ragunathan, M. Kannan, K.N. Pandiyaraj, Influence of thermal oxidation on surface and thermo-mechanical properties of polyethylene, J. Polym. Res. 18 (2011) 2175–2184. https://doi.org/10.1007/s10965-011-9628-0.
[52] L. Gardella, M. Calabrese, O. Monticelli, PLA maleation: An easy and effective method to modify the properties of PLA/PCL immiscible blends, Colloid Polym. Sci. 292 (2014) 2391–2398. https://doi.org/10.1007/s00396-014-3328-3.
[53] G. Sui, K. Wang, S. Xu, Z. Liu, Q. Zhang, R. Du, Q. Fu, The combined effect of reactive and high-shear extrusion on the phase morphologies and properties of PLA/OBC/EGMA ternary blends, Polymer (Guildf). 169 (2019) 66–73. https://doi.org/10.1016/j.polymer.2019.02.044.
[54] Y. Xia, G. Wang, Y. Feng, Y. Hu, G. Zhao, W. Jiang, Highly toughened poly(lactic acid) blends prepared by reactive blending with a renewable poly(ether□block□amide) elastomer, J. Appl. Polym. Sci. 138 (2021) 50097. https://doi.org/10.1002/app.50097.
[55] E. Alemán Espinosa, V. Escobar-Barrios, G. Palestino Escobedo, M.A. Waldo Mendoza, Thermal and mechanical properties of UHMWPE/HDPE/PCL and bioglass filler: Effect of polycaprolactone, J. Appl. Polym. Sci. 138 (2021) 1–14. https://doi.org/10.1002/app.50374.
[56] E. El-Rafey, W.M. Walid, E. Syala, A.A. Ezzat, S.F.A. Ali, A study on the physical, mechanical, thermal properties and soil biodegradation of HDPE blended with PBS/HDPE-g-MA, Polym. Bull. 79 (2022) 2383–2409. https://doi.org/10.1007/s00289-021-03623-y.
[57] M. Kumar, S. Mohanty, S.K. Nayak, M.R. Parvaiz, Effect of glycidyl methacrylate (GMA) on the thermal, mechanical and morphological property of biodegradable PLA/PBAT blend and its nanocomposites, Bioresour. Technol. 101 (2010) 8406–8415. https://doi.org/10.1016/j.biortech.2010.05.075.
[58] A. Gharehkhashli, S. Mortazavi, H. Rashidi, Photodegradation of low-density polyethylene with prooxidant and photocatalyst, J. Appl. Polym. Sci. 137 (2020). https://doi.org/10.1002/app.48979.
[59] E. Panahi, M. Gholizadeh, R. Hajimohammadi, Investigating the degradability of polyethylene using starch, oxo-material, and polylactic acid under the different environmental conditions, Asia-Pacific J. Chem. Eng. 15 (2020) 2402. https://doi.org/10.1002/apj.2402.
[60] S. Sable, S. Ahuja, H. Bhunia, Studies on Biodegradability of Cobalt Stearate Filled Polypropylene After Abiotic Treatment, J. Polym. Environ. 28 (2020) 2236–2252. https://doi.org/10.1007/s10924-020-01762-3.
[61] Z. Su, L. Zeng, S. Zhang, Q. Xu, M. Jiang, J. Liu, C. Wang, P. Liu, The effects of carbon nanotubes selective location on the structures and properties of polyphenylene sulfide/polyamide 66 fibers, J. Appl. Polym. Sci. 139 (2022) 52214. https://doi.org/10.1002/app.52214.